Low Temperature Physics/Fizika Nizkikh Temperatur, 2012, v. 38, No. 1, pp. 87–94

Low-temperature heat capacity of fullerite C_{60} doped with deuteromethane

M.I. Bagatskii, V.V. Sumarokov, and A.V. Dolbin

B. Verkin Institute for Low Temperature Physics and Engineering of the National Academy of Sciences of Ukraine
47 Lenin Ave., Kharkov 61103, Ukraine
E-mail: bagatskii@ilt.kharkov.ua

B. Sundqvist

Department of Physics, Umea University, Umea SE - 901 87, Sweden

Received June 14, 2011

The heat capacity C of fullerite doped with deuteromethane $(CD_4)_{0.4}(C_{60})$ has been investigated in the temperature interval 1.2–120 K. The contribution ΔC_{CD_4} of the CD_4 molecules to the heat capacity C has been separated. It is shown that at $T \approx 120$ K the rotational motion of CD_4 molecules in the octahedral cavities of the C_{60} lattice is weakly hindered. As the temperature decreases to 80 K, the rotational motion of the CD_4 molecules changes from weakly hindered rotation to libration. In the range $T = 1.2$–30 K ΔC_{CD_4} is described quite accurately by the sum of contributions from the translational and librational vibrations and tunneling rotation of the CD_4 molecules. The contribution of tunneling rotation to the heat capacity $\Delta C_{CD_4}(T)$ is dominant below 5 K. The effect of nuclear-spin conversion of the CD_4 molecules upon the heat capacity has been observed and the characteristic times of nuclear spin conversion between the lowest levels of the A- and T-species of the CD_4 molecules at $T < 5$ K have been estimated. A feature observed in the curve $\Delta C_{CD_4}(T)$ near $T = 5.5$ K is most likely a manifestation of a first-order phase transition in the orientational glass of the solution.

PACS: 65.40.Ba Heat capacity;
65.80.–g Thermal properties of small particles, nanocrystals, nanotubes, and other related systems;
66.35.+a Quantum tunneling of defects;
81.05.ub Fullerenes and related materials.

Keywords: heat capacity, fullerite C_{60}, rotational dynamics of CD_4.

Introduction

The discovery of new forms of carbon (fullerite, carbon nanotubes, graphene) has attracted much interest from researchers working in different fields of physics, chemistry and materials science. The interest is first of all provoked by the wide-range diversity of the physical and chemical properties of these objects. A comprehensive investigation of the physical properties of these materials is of great importance for both fundamental science and practical applications.

The thermal properties of pure fullerite have been investigated in numerous studies. Unfortunately, there have been few studies of the dynamics of impurities in C_{60} crystals.

In the low-temperature phase there is one octahedral and two tetrahedral cavities for each C_{60} molecule in the lattice. The average sizes of these are ≈ 4.12 Å and ≈ 2.2 Å, respectively [1,2]. Under certain conditions the octahedral cavities can be occupied by impurity atoms or molecules whose sizes are smaller than or similar to the size of the cavity. By now various experimental methods have been used to investigate fullerite C_{60} doped with inert gas atoms [3–8] and simple molecules [9–15] of different symmetries and sizes. Doping affects significantly the physical properties of fullerite at low temperatures [16–18].

The quantitative and qualitative features of the behavior of A_xC_{60} (A = ^{4}He, Ne, Ar, Kr, Xe) and M_xC_{60} (M = H_2, N_2, O_2, CO, CH_4, CD_4) systems depend in particular on the concentration x (x is the fraction of the octahedral cavities occupied by admixtures) and on the atomic / molecular parameters of the admixtures. Note that in a ^{4}He–C_{60} solution the ^{4}He atoms can also occupy the tetrahedral cavities. The masses, the moments of inertia, the central and

noncentral forces of the pair interaction of H_2, N_2, O_2, CO, CH_4 and CD_4 molecules are much smaller than those of C_{60} molecules. As a result, admixture of these molecules to fullerite causes comparatively weak perturbations of translational and rotational modes in the lattice [13]. On the other hand, the motion of the C_{60} molecules has an appreciable effect on the dynamics of the admixture molecules [11,13]. The lattice parameter a, the barrier ε_φ hindering the rotation of the C_{60} molecules, the temperatures of the orientational first-order phase transition T_c and of the orientational glass phase transition T_g for crystals of C_{60} doped with atomic and molecular admixtures are shown in Table 1. The admixture of the substances mentioned does not change the lattice symmetry. However, it causes a comparatively small increase in the lattice parameter a of the fullerite. As a result, the coupling energy of the C_{60} molecules and the barriers ε_φ hindering their rotation become lower. The orientational subsystem of the fullerite is more sensitive to doping. The introduced admixture lowers both the temperature of the orientational first-order phase transition T_c and the temperature of orientational glass formation T_g in fullerite (Table 1). However, within the experimental error these effects cannot be observed in solutions with the smallest gas-kinetic diameter of admixtures (^{4}He, Ne).

Table 1. Lattice parameter a, temperatures of the orientational first-order phase transition T_c and the orientational glass phase transition T_g, and the energy barrier ε_φ hindering C_{60} rotation for pure and admixture-doped fullerite

Sample	ε_φ, K	a, Å	T_c, K	T_g, K	Refs.
Pristine C_{60}	3377±116	14.161	260	90	19–21
$(^4He)_1C_{60}$*	—	14.223	246	85	22
$(^4He)_1C_{60}$	3644±348	—	260	90	19
$(Ne)_{0.49}C_{60}$	—	14.168	258	90	4,23
$(Ne)_{0.62}C_{60}$	3273±348	—	260	90	19
$(Ar)_1C_{60}$	—	14.173	251	80	6,7,22
$(Ar)_{0.49}C_{60}$	2530±174	—	247	depress	19
$(Kr)_{0.80}C_{60}$	—	14.207	238	—	7
$(Xe)_{0.66}C_{60}$	—	14.36	210	—	7
$(H_2)_1C_{60}$	—	14.17	254	90	24
$(O_2)_{0.70}C_{60}$	—	14.174	240	—	23,25
$(O_2)_{0.50}C_{60}$	2112	—	240	depress	19
$(N_2)_{0.60}C_{60}$	—	14.183	239	80	26
$(CO)_{0.67}C_{60}$	—	14.179	245	80	27–29
$(CH_4)_{0.92}C_{60}$	—	14.187	241	—	11,13

N o t e s: * in this sample the admixed ^{4}He atoms occupied both octahedral and tetrahedral cavities of fullerite [22].

Two orientational phase transitions, with $T_{c1} \approx 260$ K (as in pure C_{60}) and $T_{c2} < 260$ K, can be observed in some cases when the occupation of the cavities is incomplete ($x < 1$) [11]. The phase transitions are caused by the cooperative processes in the orientational subsystem. Thus, introduction of an admixture has a significant effect on the orientational cooperative processes in fullerite.

The low-temperature, partially orientationally-ordered SC phase of pure fullerite has two symmetrically nonequivalent states called the "pentagon" (p) and "hexagon" (h) configurations [13,30].

The energy difference between the p- and h-configurations is $\Delta E \approx 11$ meV [13,31]. The C_{60} molecules jump rapidly between the p- and h-configurations. The fraction of the p-configurations increases and the jumping velocity of the molecules decreases as the temperature is lowered.

Below the temperature of glass formation ($T_g \approx 90$ K) in fullerite C_{60} the p- and h-configurations are frozen in a ratio of about 5:1 [13,30].

Introduction of admixture atoms (molecules) changes ΔE and the fractions of the p- and h-configurations. For example, below liquid N_2 temperature the p- and h-configurations in C_{60} doped with CO are frozen randomly over the crystal in the ratio 12.5:1 [31].

Precise measurements of the thermal expansion α of C_{60} doped with atomic (He, Ne, Ar, Kr, Xe) and molecular (H_2, D_2, N_2, O_2, CO, CH_4, CD_4) admixtures in the interval T = 2–25 K have revealed a number of new effects [32–40]. The introduced admixtures change the magnitude and the temperature region of negative $\alpha(T)$. They also increase the hysteresis of the thermal expansion and bring about a maximum in the curve $\alpha(T)$ at $T \approx 5$ K. The negative thermal expansion of C_{60} at low temperatures points to a tunneling origin of the rotational states of the C_{60} molecules.

A linear contribution to the heat capacity of pure C_{60}, which is typical of glasses [41,42], was observed experimentally at $T < 3$ K [43].

The heat capacity of the interstitial solution $(N_2)_{0.2}C_{60}$ was measured in the interval T = 2–15 K using an adiabatic calorimeter [44]. It was found that the heat capacity of the solution was independent of the temperature prehistory of the sample. This means that the heat of the phase transition in the orientational glass $(N_2)_{0.2}C_{60}$ is small and does not cause hysteretic phenomena in the heat capacity (in contrast to thermal expansion [36]) in this temperature interval.

The low-temperature dynamics of the solutions $(CH_4)_xC_{60}$ and $(CD_4)_xC_{60}$ was investigated using neutron diffraction [13], NMR [11] and dilatometric [38,40] methods. The low energy part of the rotational spectrum of the nuclear spin A-, T-, and E-species of the CH_4 molecules in the octahedral cavities was specified in [13]. A nuclear spin conversion of the CH_4 molecules between the lowest levels of the A- and T-species was revealed and the corresponding time constant estimated to be $t_{1/2} \approx 2.6$ h.

The goal of this study is to investigate the low-temperature dynamics of the $(CD_4)_xC_{60}$ system by the calorimetric method.

A CD_4 molecule is a convenient admixture for this sort of studies. Since the rotational constant of the CD_4 molecule is B_{CD_4} = 3.772 K [13], the distances between the lowest energy levels of the rotational spectrum of the CD_4 molecule in the potential field of the octahedral cavity of the C_{60} lattice are equal to several degrees [13]. For this reason the contribution of the rotational motion of the CD_4 molecule to the heat capacity of the $(CD_4)_xC_{60}$ system is dominant in the region of liquid helium temperatures.

Experiment

The heat capacity C was investigated on a polycrystalline sample of the interstitial $(CD_4)_{0.40}C_{60}$ solution under constant pressure in the interval T = 1.2–120 K. Below 120 K the differences between the C-values taken at constant pressure and volume are negligible [20].

A compact adiabatic calorimeter was used to measure heat capacities of small samples of nanomaterials in the temperature interval T = 1–300 K [45,46]. The temperature of the calorimeter was measured with a CERNOX thermometer.

The temperature dependence of the heat capacity C_e of the calorimeter with adhesive but without a sample ("empty" calorimeter) was measured in an individual experiment. The use of a small quantity of the Apiezon vacuum grease allows a better thermal contact of the sample and the calorimeter. After subtracting the heat capacity of the "empty" calorimeter, the heat capacity C of the $(CD_4)_{0.40}C_{60}$ sample was normalized to unit mole of C_{60}.

The sample was a cylinder about 8 mm high and 10 mm in diameter. It was prepared by compressing ($P \approx 1$ kbar) a fullerite powder (SES, USA) C_{60} with the average crystallite size about 0.1 mm. The technique of compacting is detailed in Ref. 7. The purity of the starting fullerite C_{60} was 99.99 wt%. Before the measurement the C_{60} powder was saturated with deuteromethane for 36 h under a pressure of about 200 MPa at T = 575 °C. The procedure was performed at the Australian Nuclear Science and Technology Organisation (G.E. Gadd, S. Moricca, and D. Cassidy). The CD_4 concentration in the sample was sufficient to give about 50% occupation of the octahedral cavities in the C_{60} lattice [40].

At first the thermal expansion was investigated by the dilatometric method [40]. After completing the dilatometric investigation the sample was held for three years in a hermitized vessel filled with CD_4 gas under a pressure of ~ 1.1 atm. Before calorimetric measurement the mass of the sample was found by analytical balance weighing to be m_s = 656.68±0.05 mg. The concentration of CD_4 molecules (x = 40%) in the octahedral voids of the C_{60} lattice was found after measuring the heat capacity of the sample using a low temperature vacuum desorption gas analyzer (its design and operation are detailed in [47]).

The sample weighing and mounting in the calorimeter along with hermetization of the vacuum chamber took several hours. Then the vacuum chamber of the calorimeter was washed several times with pure nitrogen gas and the sample was held in the dynamic vacuum at room temperature for 16 h. The residual N_2 pressure in the vacuum chamber was up to several mTorrs.

The calorimeter was cooled from room temperature to ≈ 5 K through wires without using He as a heat exchanging gas. The cooling took about 10 hours. Cooling the calorimeter from 5 K to about 1.2 K and reaching a steady-state temperature rate at this temperature took about 8 hours.

The heat capacity was measured as the temperature changed at a rate of 10^{-3}–10^{-4} K/min. The increase of the sample temperature ΔT during a single measurement of the heat capacity was 5–10% of the initial temperature. The heating time t_h of the calorimeter was varied from 1 to 6 min. The effective time t_m of a single measurement of the heat capacity was $t_m = t_h + t_e$, where t_e is the time required to achieve a steady-state rate of the calorimeter temperature since the moment of switching off the heating. The time t_m varied from 10 to 4 min in the temperature region from 1.3 to 4 K, respectively. The time t_m increased with increasing temperature and was about 40 min at $T \sim 120$ K.

After the first series of heat capacity measurements at T = 1.3–6 K, the measurements were repeated several times and showed good reproducibility of the results and their independence of the temperature prehistory of the sample.

The measurement error in the heat capacity of $(CD_4)_{0.40}(C_{60})$ was 15% at T = 1.3 K, 4% at T = 2 K and about 2% at $T \geq 4$ K (for further details see [45,46]).

Results and discussion

The heat capacity C measured on a polycrystalline sample of the $(CD_4)_{0.40}(C_{60})$ solution and normalized to unit mole of C_{60} is shown in Fig. 1 along with the heat capacities C_f of pure C_{60} measured previously in the same calorimeter [45] and C_{in} determined by the intramolecular vibrations of the C_{60} molecules. C_{in} was calculated within the Einstein model using the intramolecular vibration frequencies (174 optic modes) [48–51].

The curve $C(T)$ has a minimum near T = 2.5 K (Fig. 1,*a*) which indicates that at $T < 2.5$ K the curve $C(T)$ passes through a maximum (a Schottky-type anomaly). This behavior of the temperature dependence of the heat capacity in the $(CD_4)_{0.40}(C_{60})$ solution may be attributed to the presence of a comparatively large energy gap in the low-energy part of the rotational spectrum of the CD_4 molecules. The gap separates the low-lying and high-lying levels [13]. Above 2.5 K the curve $C(T)$ grows monotonically with the temperature up to 120 K.

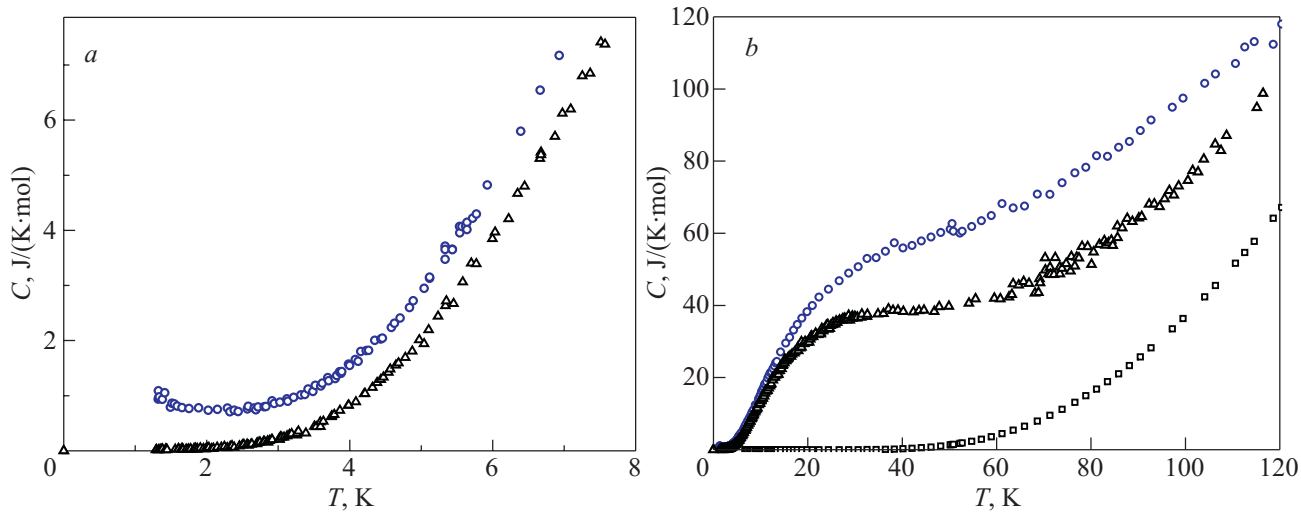

Fig. 1. Heat capacities of the solid solution C (○) and pure fullerite C_f (△) [45] normalized to unit C_{60} mole in the intervals T = 1–8 K (*a*), and 1–120 K (*b*). C_{in} is the contribution from the intramolecular vibrations of the C_{60} molecule (□).

The dependence $C(T)$ is analyzed assuming that the contributions of the rotational and translational degrees of freedom of the C_{60} and CD_4 molecules and the intramolecular degrees of freedom of the C_{60} molecule are independent of each other. In pure C_{60} the contribution ΔC_1 to the heat capacity from the rotational and translational modes of the lattice was found by subtracting C_{in} from the measured heat capacity C_f of pure C_{60} ($\Delta C_1 = C_f - C_{in}$). In the $(CD_4)_{0.40}(C_{60})$ solution, the heat capacity component ΔC_2 determined by the rotational and translational modes of the lattice and by the local translational and rotational modes of the CD_4 molecules was obtained by subtracting C_{in} from the measured heat capacity C of the solution ($\Delta C_2 = C - C_{in}$). The obtained dependences $\Delta C_1(T)$ and $\Delta C_2(T)$ are shown in Fig. 2.

It is seen in Fig. 2 that the curve $\Delta C_1(T)$ increases monotonically with temperature up to $T \approx 30$ K. On further rise of the temperature, the curve remains practically invariable and close to 5R, which is somewhat lower than the expected classical value 6R. In the region T = 3–60 K the function $\Delta C_2(T)$ grows monotonically with temperature. In the interval T = 60–90 K ΔC_2 depends weakly on temperature and above 90 K it decreases smoothly. The curve $\Delta C_2(T)$ is systematically higher than $\Delta C_1(T)$. The behavior of the dependencies $\Delta C_2(T)$ and $\Delta C_1(T)$ prompts the following qualitative conclusions: i) above 80 K the rotational motion of CD_4 molecules changes with a rising temperature from libration vibrations to a hindered rotation and the degree of attenuation of the CD_4 rotation decreases; ii) the characteristic frequencies of the local translational and librational vibrations of CD_4 molecules are higher than the frequencies of the translational and librational lattice modes of pure C_{60}.

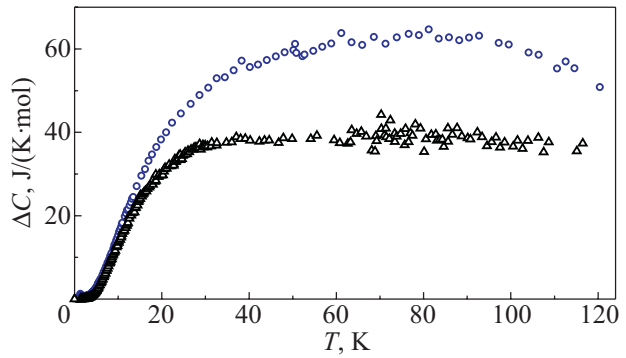

Fig. 2. The temperature dependences of the contributions to the heat capacity from: Δ — translational and rotational lattice vibrations in pure C_{60} ($\Delta C_1 = C_f - C_{in}$); ○ — translational and rotational lattice vibrations in the $(CD_4)_{0.40}(C_{60})$ solution, as well as the local translational and rotational vibrations of the CD_4 molecules ($\Delta C_2 = C - C_{in}$).

The analysis of inelastic neutron scattering data for the $(CH_4)_{0.92}(C_{60})$ and $(CD_4)_{0.88}(C_{60})$ solutions [13] prompts a conclusion that intercalation of fullerite with CH_4 and CD_4 molecules causes only a slight decrease in the frequencies of the translational and librational lattice modes. Therefore, the increase in ΔC_2 against ΔC_1 is mainly due to the rotational and translational motion of CD_4 molecules in the octahedral cavities of the C_{60} lattice. The contributions of the translational and rotational motion of the CD_4 molecules (ΔC_{CD_4}) to the heat capacity C of the solution are obtained by subtracting the measured heat capacity of pure fullerite C_f from the experimental values of the heat capacity C ($\Delta C_{CD_4} = (C - C_f)/\nu$, where ν is the number of CD_4 moles in solution). The temperature dependence $\Delta C_{CD_4}(T)$ is shown in Fig. 3 along with the calculated curves of heat capacities determined by local translational (C_{tr}) and librational (C_{lib}) vibrations of the CD_4 molecules and their tunneling rotation in the potential field of the octahedral cavities of the C_{60} lattice, for the case of an equilibrium distribution of the CD_4 nuclear-spin species ($C_{rot,\ equilib}$). The total heat capacity can be calculated as $\Delta C_{calc} = C_{tr} + C_{lib} + C_{rot,equilib}$. Here C_{tr} and C_{lib} were

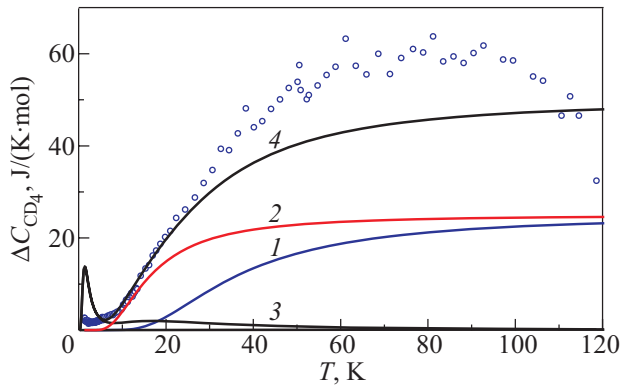

Fig. 3. The contribution ΔC_{CD_4} (○) of the CD_4 molecules to the heat capacity of the solution *C*. The calculated heat capacities are determined by local translational (C_{tr} , curve *1*) and librational (C_{lib} , curve *2*) vibrations and the tunneling rotation ($C_{rot,\ equilib}$, curve *3*) of the CD_4 molecules. $\Delta C_{calc} = C_{tr} + C_{lib} + C_{rot,equilib}$ is the calculated total heat capacity (curve *4*).

calculated within the Einstein model. C_{tr} was calculated using the characteristic Einstein temperature $\Theta_{tr} = 112.6$ K obtained from inelastic neutron scattering data [13], while the characteristic Einstein temperature $\Theta_{lib} = 51$ K used to calculated C_{lib} was found from the condition of giving the best fit to $\Delta C_{CD_4}(T)$. The calculation of $C_{rot,\ equilib}$ is described below.

It is seen that in the interval $T = 35$–110 K the calculated heat capacity $\Delta C_{calc}(T)$ is lower than $\Delta C_{CD_4}(T)$. The discrepancy may be due to "additional" local translational and rotational excitations of the CD_4 molecules. The motion of the CD_4 molecules has a comparatively weak effect on the translational and rotational lattice vibrations in the solution [13]. On the contrary, the motion of the C_{60} molecules affects appreciably the local translational and rotational vibrations of the CD_4 molecules. The formation of an orientational glass in the $(CD_4)_{0.40}(C_{60})$ solution changes the character of the rotational motion of the C_{60} molecules, which induces the "additional" local translational and rotational excitations of the CD_4 molecules.

The contribution of the tunneling rotation of CD_4 molecules dominates the heat capacity $\Delta C_{CD_4}(T)$ below 6 K. The value of $\Delta C_{CD_4}(T)$ depends on the rate of conversion of the *A*-, *T*- and *E*-nuclear spin species of the CD_4 molecules and on the effective time t_m for a single measurement of the heat capacity [52]. The influence of the conversion on the heat capacity of the solution $(CD_4)_{0.40}(C_{60})$ follows from the following facts.

1. At $T < 4$ K the average time for temperature relaxation after heating or cooling the calorimeter is about three times longer than the relaxation time in the experiment on pure C_{60}.

2. As the temperature decreases from 4 K to 1.5 K, t_m increases about twofold (from 4 to 8 min.). In pure C_{60}, the time t_m decreases.

The heat capacity $C_{rot,\ equilib}$ (for an equilibrium distribution of CD_4 species) is determined by the rotational spectrum of CD_4 molecules, which depends on the symmetry and the potential field in the lattice cavities occupied by the molecules. The value of the field depends on the fraction of C_{60} molecules in the *p*- and *h*-configurations [13].

Proceeding from the experimental data on the rotational spectrum of the *A*-, *T*- and *E*-species of CH_4 molecules in the potential field of the octahedral cavity of C_{60}, a two-parameter model of a crystal potential field $V(w) = B(CH_4)\left[\beta_4 V_4(w) + \beta_6 V_6(w)\right]$ was proposed [13], where B_{CH_4}=7.539 K is the rotational constant of the CH_4 molecule and β_4 and β_6 are dimensionless parameters. For C_{60} molecules with the *p*-configuration, the energies of some low-lying levels $E/B(CH_4) = f\left(\beta_4 = 2.1856\beta_6\right)$ of the rotational spectrum of the CH_4 molecules were calculated as a function of the potential field parameters β_4 and β_6 (see [13], Fig. 1). It is found that in the $(CH_4)_{0.92}(C_{60})$ solution the relaxation time of the occupancy of rotational energy levels above the ground state of the *A*- and *T*-species of CH_4 molecules is rather short. The time of conversion between the ground states of the *A*- and *T*-species of CH_4 molecules at $T \approx 4$ K was found to be $t_{1/2} \approx 2.6$ h [13].

Assuming that a substitution of CD_4 for CH_4 will not affect the potential field in the cavities, we renormalized the spectrum of [13] and obtained a number of low-lying levels in the rotational spectrum of the *A*-, *T*- and *E*-species of CD_4 molecules: $E\cdot(B_{CD_4}/B_{CH_4})$, where B_{CD_4} = 3.772 K is the rotational constant of the CD_4 molecule. The obtained rotational spectrum of CD_4 molecules is shown in Fig. 4. The *A*-species has the lowest energy state, therefore under the condition of equilibrium at $T = 0$ K all CD_4 molecules are in this state. At $T \neq 0$ K the equilibrium distribution of the *A*-, *T*- and *E*-species is reached through their conversion.

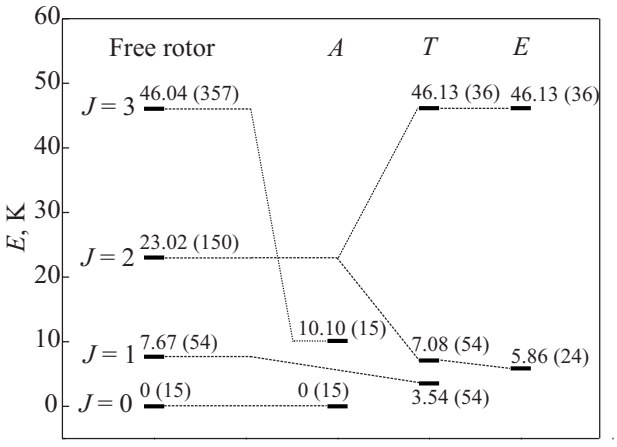

Fig. 4. The low-energy part of the rotational spectrum of free CD_4 molecules [53] and the CD_4 molecule in the potential field of the octahedral cavities in C_{60} [13] for the *A*, *T* and *E* nuclear-spin species CD_4. *J* is the rotational quantum number and *E* is the energy (the degeneracies of the levels are shown in parentheses to the right).

At $T < 6$ K the heat capacity of the $(CD_4)_{0.40}(C_{60})$ solution depends on the correlation between the characteristic conversion time τ of CD_4 molecules and the time t_m for the heat capacity measurement [52].

At $\tau << t_m$ the measured heat capacity corresponds to a near-equilibrium distribution of the nuclear spin species of CD_4 molecules.

The time of cooling the calorimeter from 5 to 1.2 K and achieving a steady-state rate of temperature was about 8 h. During this period the CD_4 species came to a near-equilibrium distribution over the sample. Most of the CD_4 molecules were in the ground state of the *A*-species. The heat capacity $\Delta C_{CD_4}(T)$ is determined by the number of CD_4 molecules which conversed during the time t_m [52]. The time constant τ for the relaxation of the CD_4 molecules to the equilibrium distribution of the nuclear spin species is described as [52]:

$$\tau = -t_m / \ln\,(1 - K^*)\,, \qquad (1)$$

where $K^* = \Delta C_{CD_4} / C_{\text{rot,equilib}}$ is the fraction of CD_4 molecules in the equilibrium distribution which changed from the ground state of the *A*-species to the ground state of the *T*-species during the time t_m.

The experimental results on the heat capacity ΔC_{CD_4} at temperatures below 10 K are shown in Fig. 5.

The rotational heat capacity C_{rot} was calculated using the spectrum of Fig. 4 with different ratios of the nuclear spin species. The calculated curves (*1–3*) are shown in Fig. 5. Curve *1* describes the rotational heat capacity $C_{\text{rot,equilib}}$ in the case of the equilibrium distribution of the nuclear spin species (the characteristic conversion time $\tau << t_m$ and the equilibrium is reached during the time t_m of one measurement run). Curve *3* presents $C_{\text{rot,high}}(T)$ on a frozen high-temperature species distribution ($x_A : x_T : x_E$ = = 15:54:12) for a free CD_4 molecule [54]. In this case $C_{\text{rot,high}} = C_{A,\text{rot}} + C_{T,\text{rot}} + C_{E,\text{rot}}$, where $C_{A,\text{rot}}$, $C_{T,\text{rot}}$ and $C_{E,\text{rot}}$ are determined only by the transitions inside each species. Curve *2* is for the case when the fraction of conversed molecules is $K^* = 1/5.8$.

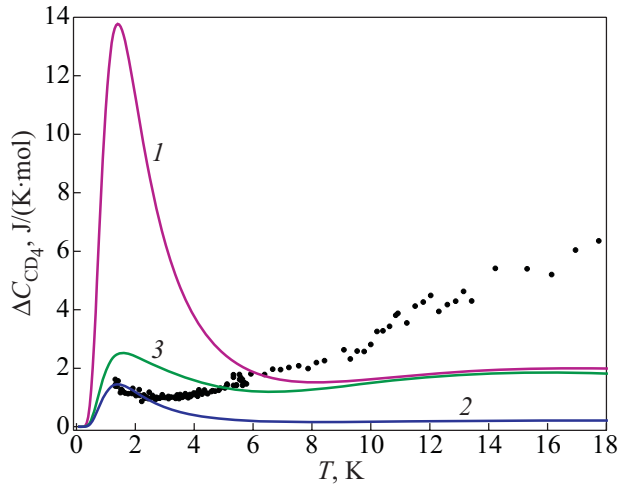

Fig. 5. The experimental temperature dependence of the heat capacity $\Delta C_{CD_4}(T)$ (●) and the calculated curves of the contributions from tunneling rotation C_{rot} to $\Delta C_{CD_4}(T)$: curve *1* ($C_{\text{rot,equilib}}$) demonstrates a case with an equilibrium distribution of CD_4 species; curve *2* a case with $K^* = \Delta C_{CD_4} / C_{\text{rot,equilib}} = 1/5.8$; curve *3* ($C_{\text{rot,high}}$) shows the result for a case with a distribution corresponding to high temperature.

It is seen in Fig. 5 that $C_{\text{rot,high}}$ (curve *3*) cannot describe the experimental dependence $\Delta C_{CD_4}(T)$ in the interval T = 1.5–5.5 K. Curve *2* describes well the experimental results below 2 K, where the rotational heat capacity is determined mainly by the changes in the occupancy of the ground states of *A*- (0 K) and *T*- (3.54 K) species during the time t_m of a single run of heat capacity measurements.

Above 5 K the heat capacity $\Delta C_{CD_4}(T)$ corresponds to the equilibrium distribution of CD_4 species.

The average values of $K^* = \Delta C_{CD_4} / C_{\text{rot,equilib}}$ were estimated at T = 2–4.5 K. The temperature dependence of the characteristic time of CD_4 conversion in the octahedral cavities of the CD_4 lattice $\tau(T)$ was calculated using Eq. (1) and experimental values of t_m (see Fig. 6).

The characteristic conversion time $\tau \approx 0.1$ h of the CD_4 molecules in the $(CD_4)_{0.40}(C_{60})$ solution at 4 K is about 25 times shorter than the conversion time $t_{1/2} \approx 2.6$ h (obtained from inelastic neutron scattering data [13]) of the CH_4 molecule in the $(CH_4)_{0.92}(C_{60})$ solution. The discrepancy suggests that at low temperatures a hybrid mechanism [55] of molecule conversion is dominant in the systems investigated, as in solid solutions of $(CH_4)_x$Kr [52,56] and $(CD_4)_x$Kr [54,57]. In Kr solutions with 5% of CD_4 and CH_4 the average conversion rate of CD_4 molecules at liquid helium temperatures is six times higher than that of the CH_4 molecules.

Hybrid [55] and quantum relaxation [58,59] mechanisms of conversion have been proposed to describe conversion in condensed systems of multiatomic molecules. According to the theory of the hybrid conversion mechanism [55], the highest conversion rate is determined simultaneously by the intramolecular magnetic interaction of

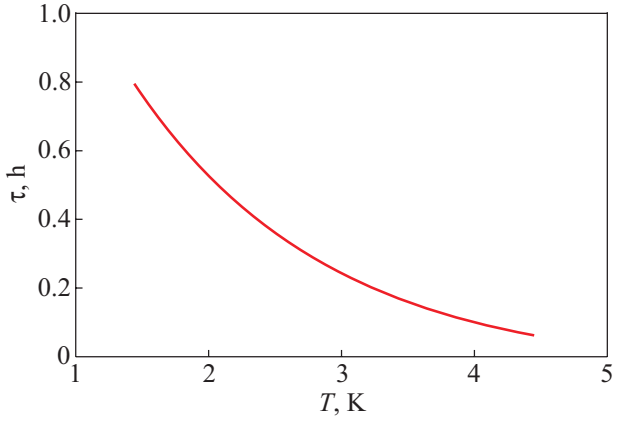

Fig. 6. Averaged characteristic conversion times $\tau(T)$ for CD_4 molecules in the octahedral cavities of the C_{60} lattice.

protons and the intermolecular noncentral interaction between the nearest molecules in the lattice. The intramolecular interaction mixes the nuclear-spin states, while the intermolecular noncentral interaction induces transitions between the rotational states transferring the conversion energy to the lattice. The hybrid mechanism is dominant at low temperatures [55]. The contribution of the quantum relaxation mechanism increases with rising temperature [58]. In this case [58] the conversion rate is determined simultaneously by the intramolecular magnetic interaction of protons and the tunnel exchange of species with equal energy levels.

The noncentral CD_4–C_{60} interaction is more intensive than the CH_4–C_{60} one. This is because the CD_4 molecule has a smaller amplitude of zero-point orientational vibrations and a larger effective electric octupole moment in the ground state. Therefore, the probability of conversion energy transfer from the CD_4 molecules to the C_{60} lattice is higher. Consequently, CD_4 molecules have a higher conversion rate.

The dependence $\Delta C_{CD_4}(T)$ has a small feature near $T = 5.5$ K. A previous study of the thermal expansion of the $(CD_4)_{0.2}(C_{60})$ and $(CD_4)_{0.5}(C_{60})$ systems at $T = 2.5$–23 K [40] revealed a first-order phase transition in the orientational CD_4–C_{60} glass in the interval 4.5–6 K. It was evident as a maximum in the curves $\alpha(T)$ at $T \approx 5$ K and a hysteresis of $\alpha(T)$. It is most likely that the feature in the curve $\Delta C_{CD_4}(T)$ near $T = 5.5$ K is a manifestation of the mentioned first-order phase transition.

Conclusions

The heat capacity of fullerite doped with deuteromethane $(CD_4)_{0.4}(C_{60})$, such that CD_4 molecules occupy 40% of the octahedral cavities in the C_{60} lattice, has been investigated for the first time in the interval 1.2–120 K.

The contribution of the local translational and rotational modes of CD_4 molecules to the heat capacity of the $(CD_4)_{0.4}(C_{60})$ solution has been separated and analyzed. It is found that above $T = 80$ K the rotational motion of the CD_4 molecules changes from libration vibrations to hindered rotation.

The effect of nuclear spin conversion on the tunneling rotation of CD_4 molecules in the octahedral cavities of the C_{60} lattice has been observed through its effect on the heat capacity. The effective characteristic times of nuclear spin conversion between the lowest levels of the *A*- and *T*-species of CD_4 molecules at temperatures below 5 K have been estimated. It is shown that a hybrid conversion mechanism is dominant in this temperature region.

It is likely that the feature detected in the curve $\Delta C_{CD_4}(T)$ near $T = 5.5$ K is a manifestation of a first-order phase transition in the orientational CD_4–C_{60} glass.

Acknowledgements

The authors are indebted to V.G. Manzhelii and A.I. Prokhvatilov for a fruitful discussion, and to G.E. Gadd, S. Moricca, and D. Cassidy for doping of a C_{60} sample with CD_4. The authors thank V.B. Esel'son and S.N. Popov for help with the work.

1. P.A. Heiney, J.E. Fischer, A.R. McGhie, W.J. Romanow, A.M. Denenstein, J.P. McCauley, Jr., A.B. Smith, III, and D.E. Cox, *Phys. Rev. Lett.* **66**, 2911 (1991).
2. R. Sachidanandam and A.B. Harris, *Phys. Rev. Lett.* **67**, 1467 (1991).
3. J.E. Schirber, G.H. Kwei, J.D. Jorgensen, R.L. Hitterman, and B. Morosin, *Phys. Rev.* **B51**, 12014 (1995).
4. B. Morosin, J.D. Jorgensen, S. Short, G.H. Kwei, and J.E. Schirber, *Phys. Rev.* **B53**, 1675 (1996).
5. G.E. Gadd, P.J. Evans, S. Moricca, and M. James, *J. Mater. Res.* **12**, 1 (1997).
6. G.E. Gadd, S.J. Kennedy, S. Moricca, C.J. Howard, M.M. Elcombe, P.J. Evans, and M. James, *Phys. Rev.* **B55**, 14794 (1997).
7. G.E. Gadd, S. Moricca, S.J. Kennedy, M.M. Elcombe, J. Evans, M. Blackford, D. Cassidy, C.J. Howard, P. Prasad, J.V. Hanna, A. Burchwood, and D. Levy, *J. Phys. Chem. Solids* **58**, 1823 (1997).
8. M. Gu and T.B. Tang, *J. Appl. Phys*. **93**, 2486 (2003).
9. J.E. Schirber, R.A. Assink, G.A. Samara, B. Morosin, and D. Loy, *Phys. Rev*. **B51**, 15552 (1995).
10. S.A. Meyers, R.A. Assink, J.E. Schirber, and D. Loy, *Mater. Res. Soc. Symp. Proc.* **359**, 505 (1995).
11. B. Morosin, R.A. Assink, R.G. Dunn, T.M. Massis, and J.E. Schirber, *Phys. Rev.* **B56**, 13611 (1997).
12. M. James, S.J. Kennedy, M.M. Elcombe, and G.E. Gadd, *Phys. Rev.* **B58**, 14780 (1998).
13. G.H. Kwei, F. Troun, B. Morosin, and H.F. King, *J. Chem. Phys*. **113**, 320 (2000).
14. S.A. FitzGerald, T. Yildirim, L.J. Santodonato, D.A. Neuman, J.R.D. Copley, J.J. Rush, and F. Trouw, *Phys. Rev.* **B60**, 6439 (1999).
15. I. Holleman, G. von Helden, A. van der Avoird, and G. Meijer, *Phys. Rev. Lett.* **80**, 4899 (1998).
16. B. Sundqvist, *Adv. Phys*. **48**, 1 (1999).
17. B. Sundqvist, *Fiz. Nizk. Temp*. **29**, 590 (2003) [*Low Temp. Phys*. **29**, 440 (2003)].
18. T.L. Makarova, *Semicond.* **35**, 243 (2001).
19. T.B. Tang and M. Gu, *Fiz. Tverd. Tela* **44**, 607 (2002).
20. N.A. Aksenova, A.P. Isakina, A.I. Prokhvatilov, and M.A. Strzhemechny, *Fiz. Nizk. Temp*. **25**, 964 (1999) [*Low Temp. Phys*. **25**, 784 (1999)].
21. M.I.F. David, R.M. Ibberson, T.J.S. Dennis, J.P. Hare, and K. Prassides, *Europhys. Lett.* **18**, 219 (1992).
22. Yu.E. Stetsenko, I.V. Legchenkova, K.A. Yagotintsev, A.I. Prokhvatilov, and M.A. Strzhemechny, *Fiz. Nizk. Temp*. **29**, 597 (2003) [*Low Temp. Phys*. **29**, 445 (2003)].
23. M. Gu and T.B. Tang, *J. Appl. Phys.* **93**, 2486 (2003).

24. K.A. Yagotintsev, Yu.E. Stetsenko, I.V. Legchenkova, A.I. Prokhvatilov, and M.A. Strzhemechny, E. Schafler, and M. Zehetbauer, *Fiz. Nizk. Temp*. **35**, 315 (2009) [*Low Temp. Phys*. **35**, 238 (2009)].
25. B. Renker, H. Schober, M.T. Fernandez-Diaz, and R. Heid, *Phys. Rev*. **B61**, 13960 (2000).
26. N.N. Galtsov, A.I. Prokhvatilov, and G.N. Dolgova, D. Cassidy, G.E. Gadd, and S. Moricca, *Fiz. Nizk. Temp*. **33**, 1159 (2007) [*Low Temp. Phys*. **33**, 881 (2007)].
27. I. Holleman, G. von Helden, E.H.T. Olthof, P.J.M. van Bentum, R. Engeln, G.H. Nachtegaal, A.P.M. Kemtgens, B.H. Meier, A. van der Avoird, and G. Meijer, *Phys. Rev. Lett*. **79**, 1138 (1997).
28. Sander van Smaalen, R. Dinnebier, I. Holleman, G. Helden, and G. Meijer, *Phys. Rev.* **B57**, 6321 (1997).
29. Iwan Holleman, *Dynamics of* CO *in Solid* C_{60}, *Thesis Katholieke Universiteit Nijmegen* (1998) (in Dutch).
30. W.I.F. David, R.M. Ibberson, T.J.S. Dennis, J.P. Hare, and K. Prassides, *Europhys. Lett*. **18**, 219 (1992).
31. S. van Smaalen, R. Dinnebier, I. Holleman, G. von Helden, and G. Meijer, *Phys. Rev*. **B57**, 6321 (1998).
32. A.N. Aleksandrovskii, V.G. Gavrilko, V.B. Esel'son, V.G. Manzhelii, B.G. Udovidchenko, V.P. Maletskiy, and B. Sundqvist, *Fiz. Nizk. Temp.* **27**, 1401 (2001) [*Low Temp.Phys.* **27**, 1033 (2001)].
33. A.N. Aleksandrovskii, V.G. Gavrilko, V.B. Esel'son, V.G. Manzhelii, B. Sundqvist, B.G. Udovidchenko, and V.P. Maletskiy, *Fiz. Nizk. Temp.* **27**, 333 (2001) [*Low Temp. Phys.* **27**, 245 (2001)].
34. A.N. Aleksandrovskii, A.S. Bakai, A.V. Dolbin, G.E. Gadd, V.B. Esel'son, V.G. Gavrilko, V.G. Manzhelii, B. Sundqvist, and B.G. Udovidchenko, *Fiz. Nizk. Temp.* **29**, 432 (2003) [*Low Temp. Phys.* **29**, 324 (2003)].
35. A.N. Aleksandrovskii, A.S. Bakai, D. Cassidy, A.V. Dolbin, V.B. Esel'son, G.E. Gadd, V.G. Gavrilko, V.G. Manzhelii, S. Moricca, and B. Sundqvist, *Fiz. Nizk. Temp.* **31**, 565 (2005) [*Low Temp. Phys.* **31**, 429 (2005)].
36. V.G. Manzhelii, A.V. Dolbin, V.B. Esel'son, V.G. Gavrilko, D. Cassidy, G.E. Gadd, S. Moricca, and B. Sundqvist, *Fiz. Nizk. Temp.* **32**, 913 (2006) [*Low Temp. Phys.* **32**, 695 (2006)].
37. N.A.Vinnikov, V.G. Gavrilko, A.V. Dolbin, V.B. Esel'son, V.G. Manzhelii, and B. Sundqvist, *Fiz. Nizk. Temp.* **33**, 618 (2007) [*Low Temp. Phys.* **33**, 465 (2007)].
38. A.V. Dolbin, V.B. Esel'son, V.G. Gavrilko, V.G. Manzhelii, N.A. Vinnikov, G.E. Gadd, S. Moricca, D. Cassidy, and B. Sundqvist, *Fiz. Nizk. Temp.* **33**, 1401 (2007) [*Low Temp. Phys.* **33**, 1068 (2007)].
39. A.V. Dolbin, V.B. Esel'son, V.G. Gavrilko, V.G. Manzhelii, N.A. Vinnikov, G.E. Gadd, S. Moricca, D. Cassidy, and B. Sundqvist, *Fiz. Nizk. Temp.* **34**, 592 (2008) [*Low Temp. Phys.* **34**, 470 (2008)].
40. A.V. Dolbin, N.A. Vinnikov, V.G. Gavrilko, V.B. Esel'son, V.G. Manzhelii, G.E. Gadd, S. Moricca, D. Cassidy, and B. Sundqvist, *Fiz. Nizk. Temp.* **35**, 299 (2009) [*Low Temp. Phys.* **35**, 226 (2009)].
41. U.T. Hochli, K. Knorr, and A. Loidl, *Adv. Phys.* **39**, 405 (1990).
42. V.G. Manzhellii, M.I. Bagatskii, I.Ya. Minchina, and A.N. Aleksandrovskii, *J. Low Temp. Phys.* **111**, 257 (1998).
43. W.P. Beyermann, M.F. Hundley, J.D. Thompson, F.N. Diederich, and G. Grüner, *Phys. Rev. Lett*. **68**, 2737 (1992).
44. A.M. Gurevich, A.V. Terekhov, D.S. Kondrashev, A.V. Dolbin, D. Cassidy, G.E. Gadd, S. Moricca, and B. Sundqvist, *Fiz. Nizk. Temp.* **32**, 1275 (2006) [*Low Temp. Phys*. **32**, 967 (2006)].
45. M.I. Bagatskii, V.V. Sumarokov, and A.V. Dolbin, *Fiz. Nizk. Temp.* **37**, 535 (2011) [*Low Temp. Phys.* **37**, 424 (2011)].
46. M.I. Bagatskii, V.V. Sumarokov, A.V. Dolbin, V.G. Manzhelii, and B. Sundqvist, in: *Abstracts 2th Int. Conf. "Nanostructure materials-2010: Belarus–Russia–Ukraine"*, Kiev, Ukraine (2010), p. 464.
47. A.M. Aleksandrovskii, M.A. Vinnikov, V.G. Gavrilko, O.V. Dolbin, V.B. Esel'son, and V.P. Maletskiy, *Ukr. J. Phys.* **51**, 1152 (2006).
48. J. Mooij, *The Vibrational Spectrum of Buckminsterfullerene, Master's Thesis in Mathematics*, Katholieke Universiteit Nijmegen (2003).
49. D.E. Weeks and W.G. Harter, *J. Chem. Phys.* **90**, 4744 (1989).
50. D.S. Bethune, G. Meijer, W.C. Tang, H.J. Rosen, W.G. Golden, H. Seki, C.A. Brown, and M.S. de Vries, *Chem. Phys. Let*. **179**, 181 (1991).
51. V. Schettino, M. Pagliai, L. Ciabini, and G. Cardini, *J. Phys. Chem*. **A105**, 192 (2001).
52. M.I. Bagatskii, V.G. Manzhelii, I.Ya. Minchina, D.A. Mashchenko, and I.A. Gospodarev, *J. Low Temp. Phys*. **130**, 459 (2003).
53. E.B. Wilson, *J. Chem. Phys.* **3**, 276 (1935).
54. M.I. Bagatskii, V.G. Manzhelii, D.A. Mashchenko, and V.V. Dudkin, *Fiz. Nizk. Temp*. **29**, 216 (2003) [*Low. Temp. Phys.* **29**, 159 (2003)].
55. A.J. Nijman and A.J. Berlinsky, *Canad. J. Phys*. **58**, 1049 (1980).
56. I.Ya. Minchina, M.I. Bagatskii, V.G. Manzhelii, O.V. Sklyar, D.A. Mashchenko, and M.A. Pokhodenko, *Fiz. Nizk. Temp*. **27**, 773 (2001) [*Low Temp. Phys.* **27**, 568 (2001)].
57. M.I. Bagatskii, V.G. Manzhelii, V.V. Dudkin, D.A. Mashchenko, and S.B. Feodosyev, *Fiz. Nizk. Temp*. **29**, 1352 (2003) [*Low. Temp. Phys*. **29**, 1028 (2003)].
58. R.F. Curl, J.V.V. Kasper, and K.S. Pitzer, *J. Chem. Phys*. **46**, 3220 (1967).
59. P.L. Chapovssky and L.J.F. Hermans, *Annu. Rev. Phys. Chem.* **50**, 315 (1999).